WCTE 2016
World Conference on Timber Engineering
August 22-25, 2016 | Vienna, Austria

TWO-WAY SPANNING CLT-CONCRETE-COMPOSITE-SLAB

Stefan Loebus[1], Stefan Winter[2]

ABSTRACT: This paper examines the load-bearing behaviour of cross-laminated-timber-concrete-composite slabs. The inhomogeneous distributed orientation of the trajectories of principal stress within the slab effected the design of the shear connection between the cross-laminated-timber (CLT) and concrete layer. Two well-known shear connection types, fully threaded screws in an angle of 45° and rectangular milled in notches, were examined in bi-axially loaded push out tests. Natural frequency tests and medium-scale test including the two shear connection types and different CLT-layer configurations determined the effective bending stiffness of the slab and the effective torsional bending stiffness of the slab respectively. The results facilitate the description of the bi-axial load-bearing behaviour, and establish a basis for a structural design model in two-way spanning CLT-concrete-composite-slab engineering. The paper eventually suggests first calculation models, a simplified FEM-model and a grid model. In this regard, a force-fitting element joint was developed and tested for practical reasons.

KEYWORDS: CLT, TCC, two-way spanning slab, shear connection, notch, fully threaded screw, natural frequency, effective bending stiffness, torsional bending stiffness, push-out test, force-fitting element joint

1 INTRODUCTION

Both, CLT (Cross-Laminated Timber) and TCC (Timber-Concrete-Composite) are technologies that have evolved effectively in the recent years. CLT enabled large areal timber structures with a bi-axial load-bearing capacity. TCC enhanced conventional slabs by improving load-bearing capacity, acoustics, and fire safety properties. These slabs have been applied in renovation and modern (timber) buildings, but are still limited to a one-way spanning system. By combining CLT and TCC, a two-way spanning slab becomes possible with an improved load-bearing behaviour, furthermore offering flexible solutions regarding the positioning of supporting walls and columns.

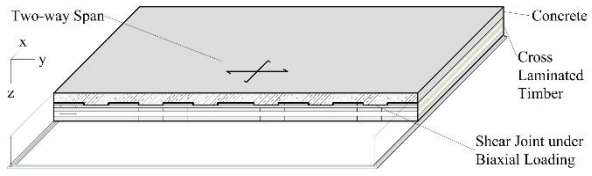

Figure 1: *CLT-Concrete-Composite-Slab*

2 SCHEMATIC LOAD-BEARING BEHAVIOUR

Looking at the trajectories of principal stress within a structural plate may help to understand the main investigative questions regarding a two-way spanning slab compared to a known and working one-way spanning concept. Figure 3 and 4 schematically compare the trajectories for two-plate-configurations. In an one-way spanning TCC-system the interplay of concrete stiffness (EI_C), CLT stiffness ($B_{CLT,x}$ and S_x) and shear connection stiffness (K_x) happens unidirectionally and is summarized with B_x. Here the direction of principal stress always runs perpendicular to the support lines. In a two-way spanning plate system, the trajectories of principal stress do not follow just one direction. The direction depends on load application, support type and stiffness distribution within the plate. For an approximate determination of the stress distribution, all stiffness are summarized in the effective bending stiffness B_x and B_y and the effective torsional bending stiffness B_{xy}. These three parameters are utilized to predict the proportion of activation of the second way (in Y) in a two-way spanning plate.

[1] Stefan Loebus, Research Associate, Chair for Timber Structures and Building Construction, Technische Universität München, Arcisstr. 21, Munich, Germany. Email: loebus@tum.de

[2] Stefan Winter, Professor, Chair for Timber Structures and Building Construction, Technische Universität München, Arcisstr. 21, Munich, Germany. Email: winter@tum.de

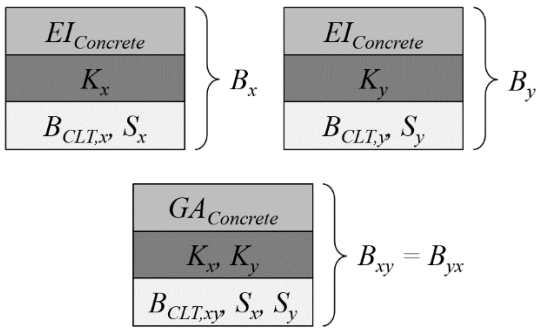

Figure 2: *Effective stiffness B summarizing the stiffness properties of concrete, shear connection, and CLT*

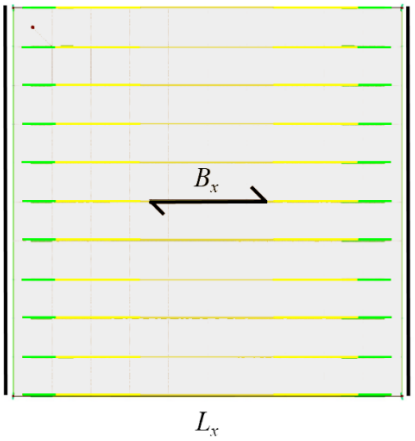

Figure 3: *One-way spanning: Schematic view of trajectories of principal stresses depending on effective stiffness and loading bearing direction*

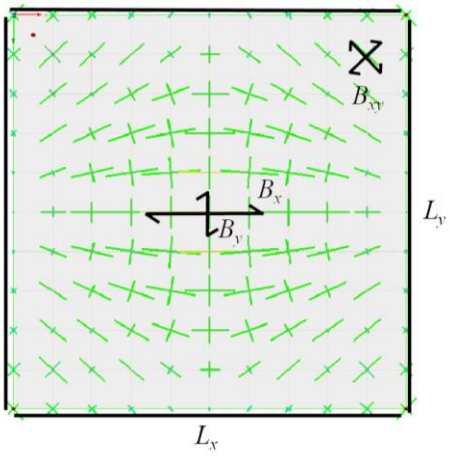

Figure 4: *Two-way-spanning: Schematic view of trajectories of principal stresses depending on effective stiffness and loading bearing direction*

3 EXPERIMENTAL EXAMINATION OF THE LOAD-BEARING BEHAVIOUR

3.1 SET BOUNDARIES

Due to the many relevant parameters influencing the load-bearing behaviour of the composite-slab, several boundaries were set prior to the examinations:

- *Concrete:* Strength class C20/25; very pourable (>F5); Minimum reinforcement Q188A; layer thickness t_c = 80 mm.
- *CLT:* Strength class C24; no edge bonding; individual layer thickness $t_{CLT,i}$ = 20/30/40 mm; 5 layers.
- *Shear connection type:*
  - Notch: rectangular; non-reinforced
  - Screw: fully-threaded; screwing angle 45°; (Wuerth Assy Plus SK Ø8-L160 mm).
- *Separation layer between concrete and timber:* none.
- *Support:* Hinged support on all sides; Non-/hold against lifting.
- *Side length ratio:* L_y / L_x = 1.0 ~ 1.5.

3.2 SHEAR CONNECTION - *K*

The shear connection stiffness is a predominant factor for the load-bearing and deformation behaviour of TCC-construction, hence necessitating an examination of the connection behaviour in a two-way spanning system. As described in Chapter 2, the trajectories follow different directions. To activate the maximum load bearing potential it is necessary to align the shear connection to the principal stress. Note, that a change of load distribution (e.g. from full to half sided) consequently alters the direction of the trajectories of principal stress as well. In practice, a deviation from the fixed connection position is always possible. β describes the deviation angle. The angle α between grain directions to principal shear force considers an influence of the (orthotropic) CLT-layers grain direction on the shear connection behaviour. (See figure 5 and 6).

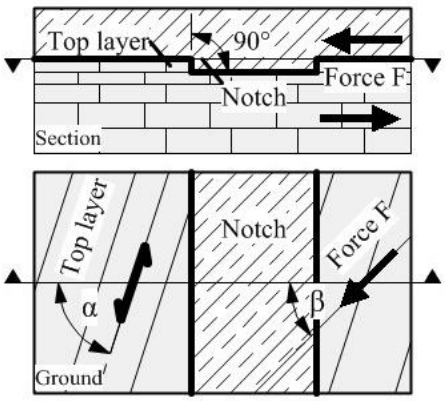

Figure 5: *Shear connection alignment: Notch*

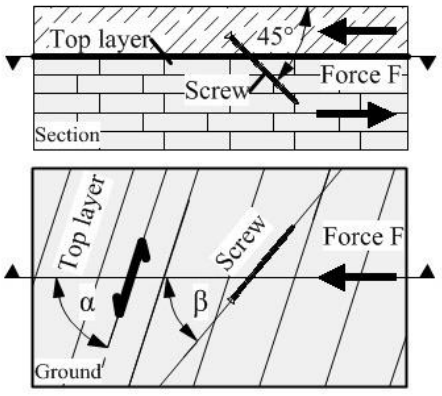

Figure 6: *Shear connection alignment: Screw*

Table 1 describes the examination of different directions of principal stress and resulting adaption of the shear connection in the setup. Questions remain how shear connection stiffness and load bearing capacity behave, if a) the fastener is turned in plate-plane and deviates from its original orientation to grain direction, and b) the shear load direction deviates from the shear connection.

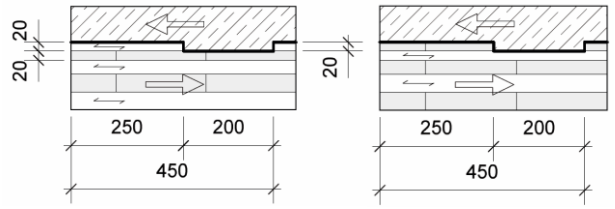

Figure 7: *Shear Connection: Notch Type 1 in X with α = 0° analogue [1] (left) and Notch Type 1 in Y with α = 90° (right)*

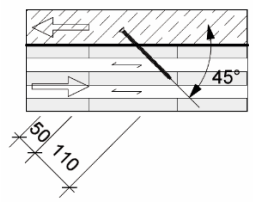

Figure 8: *Shear Connection: Screw Type 1*

Table 1: *Results to Push-Out-Tests with TCC-Shear-Connections*

Shear Connection	α	β	$t_{concrete}$*	$F_{max,mean}$	CV(F)	$k_{s,mean}$	CV(k_s)
Notch	[°]	[°]	[d]	[kN/m]	[%]	[kN/mm/m]	[%]
Type 1	0	0	17	344.7	6.5	676.5	30.1
Type 1	0	0	120	370.5	1.6	759.5	25.3
Type 1	90	0	17	97.4	3.5	134.0	15.6
Type 1	90	0	120	124.7	4.8	83.1	5.1
Screw	[°]	[°]	[d]	[kN/Stk]	[%]	[kN/mm/Stk]	[%]
Type 1	0	0	17	21.1	2.0	80.3	15.5
Type 1	0	0	120	21.8	10.8	41.9	7.2
Type 1	0	30	17	19.1	4.6	54.8	30.3
Type 1	0	30	120	20.1	1.9	18.9	17.7
Type 1	0	60	17	14.7	9.2	47.1	38.6
Type 1	0	60	120	15.4	1.4	7.1	16.4

**The first test was conducted after $t_{concrete}$=17 d with reaching the minimum strength C20/25. The top CLT-layer showed a relatively high moisture (~25%). After $t_{concrete}$=120 d the test was conducted again with reduced wood moisture*

Regarding the notch, the test results reveal a large descent in load bearing capacity and an even larger loss in stiffness with increasing angle α. Therefore, an adaption of the notch is necessary. The failure picture in figure 10 shows that due to the low young's modulus perpendicular to the grain, the stress dissipates to the next layer within a timber length of l_v ~ 75 mm in front of the notch. Consequently, it is feasible to reduce notch length and timber length in front of notch and thereby increase the number of notches per unit length (figure 12).
Figure 13 depicts another alternative with bypassing the top "weak" layer (α = 90°) and embedding the notch in the second "strong" layer (α = 0°).
With an angle α = 90° in the second layer, rolling shear failure occurs, see figure 10 right. Limiting the notch depth t < top layer thickness $t_{CLT,1}$ reduces the shear stress in the second layer (with α = 0°) by strapping back parts of the layer below the notch and hence increasing the shear transmission area (comparison of figure 7 left and figure 11). To keep the *t/l*-ratio of the concrete console in an appropriate level, it is recommended to apply a slender top timber layer.

The tested screw shear connections, listed in table 1, yielded a low decrease in load-bearing capacity while stiffness considerably decreased depending on the force-screw angle β. The specimens with screws aligned correspondent to the trajectories of principal stress revealed an even and therefore optimum stiffness distribution in the composite connection (figure 17).

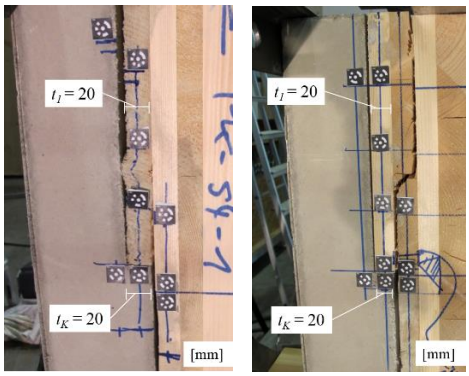

Figure 10: *Push-Out-Test Result: Notch Type 1 in X (left) and in Y (right)*

Figure 9: *Push-Out-Test Result: Screw Type 1*

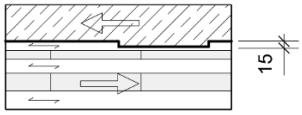

Figure 11: *Improved notch configuration: Notch Type 2 and 3 in X*

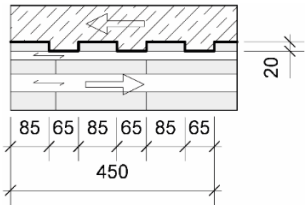

Figure 12: *Improved notch configuration: Notch Type 2 in Y*

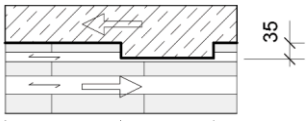

Figure 13 *Improved notch configuration: Notch Type 3 in Y*

3.3 TORSION IN PLATES – B_{xy}

Besides the load bearing behaviour in primary and secondary direction, the torsional bending behaviour is the third component for the description of the plate load bearing behaviour. A static four-sided plate experiences its main torsional bending in the corners. In general, torsional bending and bending load are blended. A pure torsional bending load is created with the respective deformation form (figure 14). This leads to the grid model in figure 15 and onward to test setup in figure 19.

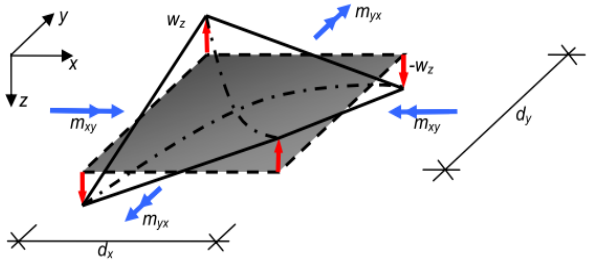

Figure 14: *Deformation of a plate section under pure torsional bending [1]*

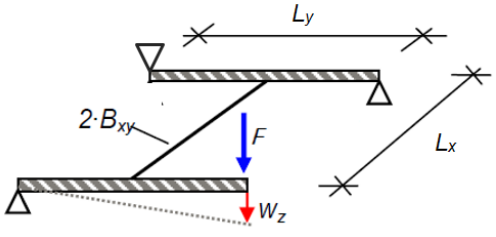

Figure 15: *Grid model according to [1] with $B_{xy} = B_{yx}$*

The results of the above described shear connection tests induced the order and alignment of the shear connections. The notches (Type 3 from figure 12 and 13) directed parallel to the plate sides in orthogonal lines, which facilitated the grooving process. The screws followed the trajectories of principal stress. For practical reasons, the screw alignment in plane was discretised in steps of 22.5° (figure 17). The CLT-layer configuration followed (1) a minimal configuration, (2) the layer specification by the notch, and (3) a standard configuration with even layers (table 2).

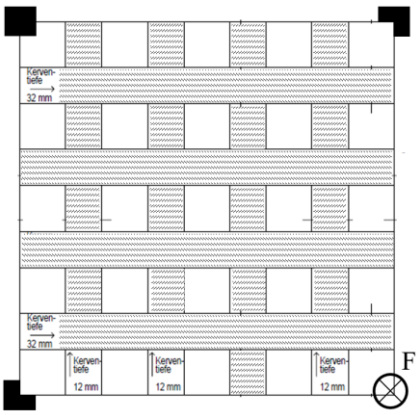

Figure 16: *Torsional bending specimen with orthogonal notch alignment*

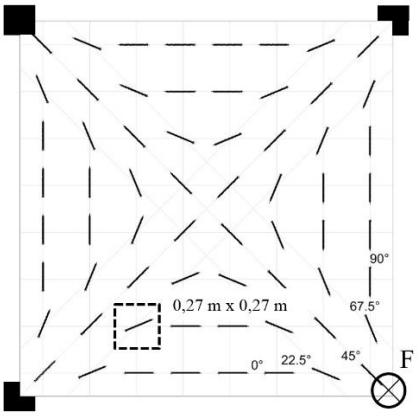

Figure 17: *Torsional bending specimen with screw alignment to trajectories of principal stress*

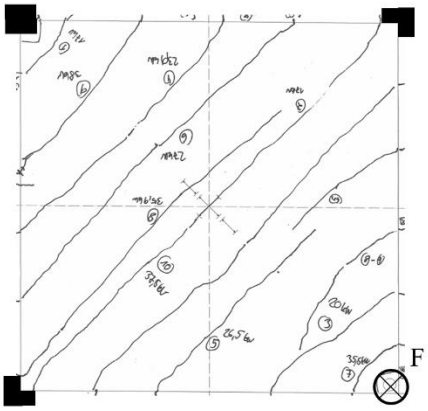

Figure 18: *Torsional bending test result showing concrete surface after loading with force F*

None of the specimens reached its ultimate load due to the large deflection w_z. Abort criterion in all cases was a deflection at the load application point $w_{max} > 50$ mm. All specimens showed a linear-elastic modulus of displacement until a combination of tension and shear-tension crack on the upper side of the concrete layer occurred (figure 18). The modulus of displacement corresponded to the torsional bending stiffness B_{xy} (table 2)

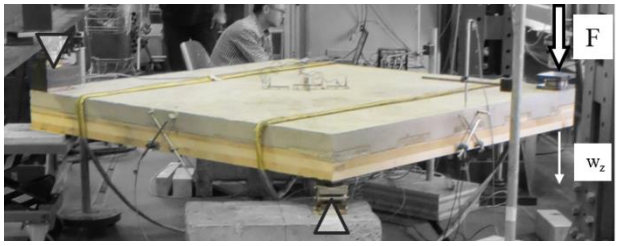

Figure 19: *Torsional bending test setup with specimen L_x x L_y = 2.05 m x 2.05 m (compare to Figure 15)*

3.4 NATURAL FREQUENCY TESTS – B_x, B_y

Additional to the force-displacement-tests for determination of torsional stiffness B_{xy}, natural frequency test were performed on the same specimens to determine the corresponding bending stiffness B_x and B_y. The point supports placed in the inflexion points of each eigenmode enabled a free oscillation of the compact slabs (with *h/l*-ratio 8.5 to 10.0)—. For better identification, the eigenmodes and natural frequencies were calculated accordingly in a FEM-volume model (depict in figure 21). Comparing the measured frequency spectrum with the FEM-calculation identified the relevant modes.

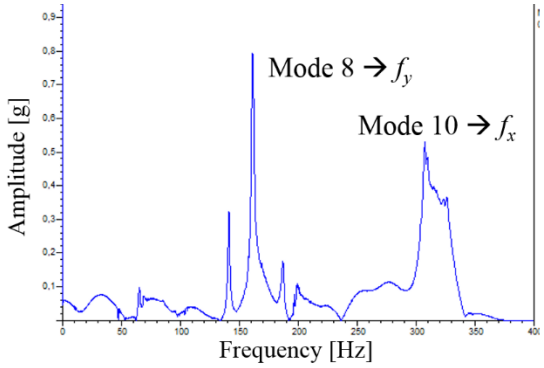

Figure 20: *Exemplary frequency spectrum of natural frequency test*

Table 2: *Effective (torsional) bending stiffness before concrete cracking*

Shear Connection	CLT	$B_{x,mean}$	$CV(B_x)$	$B_{y,mean}$	$CV(B_y)$	$B_{xy,mean}$	$CV(B_{xy})$
	[mm]	[kNm²/m]	[%]	[kNm²/m]	[%]	[kNm²/m]	[%]
Notch Type 3	‖20⊥20‖40⊥40‖40	10.5	1.9	8.16	1.4	3.05	5.0
Notch Type 3	‖20⊥20‖40⊥40	5.71	4.7	7.98	2.8	2.33	8.5
Screw Type 1	‖20⊥20‖40⊥40‖40	8.97	2.4	5.77	2.0	2.38	3.3
Screw Type 1	‖30⊥30‖30⊥30‖30	10.42	2.4	7.14	4.5	2.53	6.0

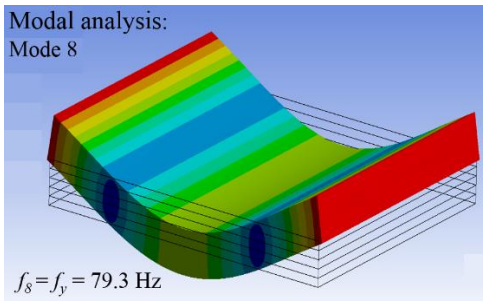

Figure 21: *FEM-simulation (ANSYS) for eigenmode determination analogue the first bending beam eigenmode "free – free"*

The effective bending stiffness B can be derived from the natural frequency of a freely supported beam:

$$B = \frac{4 \cdot \pi^2 \cdot f^2 \cdot \rho \cdot A \cdot L^4}{(\gamma_k \cdot L)^4} \quad (1)$$

In equation (1), L is the side length, $\rho \cdot A \cdot L$ the total weight and $(\gamma_k \cdot L)^2$ the first eigenmode coefficient.

3.5 Comparison

In a first comparing grid model calculation, the influence of the evaluated torsional bending stiffness B_{xy} was compared with the bending stiffness B_x and B_y. By comparing $B_{xy,grid} = B_{xy,test}$ with $B_{xy,grid} = 0$, the reduction of the torsional bending stiffness resulted in an increase of the deflection w_{max} and of the bending moments $m_{x,max}$ and $m_{y,max}$ by approximately 14 %. With a proportion $L_y/L_x > 1$, the influence of the torsional bending stiffness further decreased.

4 FORCE-FITTING ELEMENT JOINT

As transportation and production limit the slab element size, a force-fitting element joint is necessary to activate the biaxial load-bearing capacity. Most important parameter is the effective bending stiffness of the joint connection. A loss in stiffness reduces the stiffness of the bearing axis orthogonal to the joint line and therefore a balanced biaxiality.

With glued-in reinforcement bars, a connection was developed, which meets the requirements of stiffness and practical buildability (see ***Figure 22***) [5].

Figure 22: *Element connection with glued-in reinforcement bars. To activate the force-fit, concrete is poured into the gap.*

In four-point bending tests the specimen with joint and depict connection showed a nearly equal deflection in comparison to the specimen without joint (Figure 23). Hence, the application of this element connection does not result in stiffness loss.

Figure 23: *Four-point bending test on jointed CLT-TCC-elements*

5 CALCULATION MODEL

5.1 General

Parallel to the experimental studies, calculation methods were developed. The holistic study of the plate within a vast solid model with individual modelling of the connections and incorporating non-linear material behaviour is very complex and computationally intensive. Therefore two simplified models were developed, which could be validated for practical calculation and design of two-way spanning TCC-slabs.

5.2 Simplified Solid-Model

The concrete- and CLT-layers were modelled individually. All contacts between the layers were defined as rigid. The shear connections were not modelled. The shear connection stiffness *K* was "smeared"

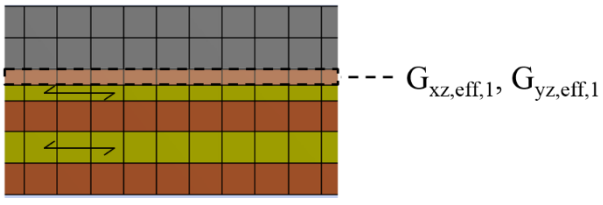

Figure 24: *Modified top CLT layer in FEM-solidmodel*

over the complete joint area and was taken into account by modifying the shear modulus of the top timber layer (figure 24: $G_1 \rightarrow G_{eff}$).

$$G_{eff,1} = \frac{t_1}{\frac{1}{K} + \frac{t_1}{G_1}} \qquad (2)$$

5.3 Grid Model

To calculate the local effect of shear connections, a spatial grid model in imitation of [4] was developed to enable individual modelling of shear connections. Besides the possibility to give a shear connection a local geometric orientation, the degree of composite and the load distribution in the model can be evaluated.

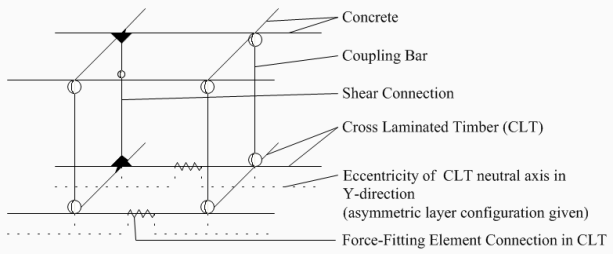

Figure 25: *Three dimensional grid model approach*

6 CONCLUSION

The executed experiments provide a good basis for the description of the load bearing behaviour of two-way spanning cross-laminated timber concrete composites. Important parameters like the shear connection stiffness and the torsional bending stiffness were quantified. Supplementing tests on larger scaled slabs could validate the calculation models. In the area of shear connections, solutions to the biaxial stiff execution have been presented. A notch construction was investigated, which exhibited a high shear stiffness in both axis ways. The calculation and production effort for a spatial distributed screw alignment is arguable, but may be adequate in local applications.

Future parameter studies are needed to show limits and potential of the structural system. Influences as adhesion and moisture interaction have an unneglectable impact on the composite behaviour, and are object of further investigations. In principal, further discussion is needed about the degree of implication of the adhesion in the ultimate and serviceability limit state.

REFERENCES

[1] Michelfelder B.: Trag- und Verformungsverhalten von Kerven bei Brettstapel-Beton-Verbunddecken, Universität Stuttgart, Stuttgart, Germany, 2006.

[2] DIN EN 26891: Timber structures – Joints made with mechanical fasterners – Gerneral principles for the determination of strength and deformation characteristics, DIN Deutsches Institut für Normung e.V., 1991.

[3] Mestek P.: Punktgestützte Flächentragwerke aus Brettsperrholz (BSP) – Schubbemessung unter Berücksichtigung von Schubverstärkungen, Technische Universität München, Munich, Germany 2011.
[4] Grosse M., Hartnack R., Lehmann S., Rautenstrauch K.: Modellierung von diskontinuierlich verbundenen HolzBetonVerbundkonstruktionen / Teil 1: Kurzzeittragverhalten, Bautechnik, Volume 10 Issue 8, 2003.
[5] Lechner, M: Kraftschlüssiger Brettsperrholz-Beton-Verbundstoß, Master‘s Thesis, Technische Universität München, Munich, Germany 2016.